Fundamental Studies of the Energetics and Dynamics of State-Selected Co^+ Reacting with CH_3I. The Co^+–CH_3 and Co^+–I Bond Energies

Petra A. M. van Koppen,* Paul R. Kemper, and Michael T. Bowers*

Contribution from the Department of Chemistry, University of California, Santa Barbara, California 93106

Received December 7, 1992

Abstract: The a^3F, a^5F, and b^3F states of Co^+ react with CH_3I to form the $CoCH_3I^+$ adduct as well as $CoCH_3^+ + I$ and $CoI^+ + CH_3$ products. The observed rates for adduct formation and methyl elimination were found to be strongly dependent on the electronic configuration of the metal ion. Under our experimental conditions (10^{-5} Torr of CH_3I in 1.75 Torr of He), adduct formation is the dominant product for the a^3F $3d^8$ ground state of Co^+, with only small amounts of elimination products observed. The $4s3d^7$ excited states (a^5F and b^3F) show greatly reduced clustering (due to the repulsive 4s electron) and enhanced elimination channels. The temperature dependencies of the rate constants were measured and indicate that all reaction channels, for ground and excited state Co^+, involve the formation of a complex as the initial step in the reaction. By modeling the reaction efficiencies for the elimination channels on the ground-state surface with statistical phase space theory, the Co^+–CH_3 and Co^+–I bond energies were determined to be $D°_0 = 53.3 \pm 2$ and 50.6 ± 2 kcal/mol, respectively.

Introduction

Studies of gas-phase ion–molecule reactions involving atomic transition metal ions have provided detailed insight into their mechanisms and energetics.[1-3] These reactions have been shown to be generally complex and usually extremely dependent on the electronic state of the metal ion.[4-16] Characterizing the effects of the metal ion electronic state is therefore especially important in transition metal ion reactions.

Several studies of atomic metal ions with alkyl halides have been reported. In one of the first studies, Allison and Ridge[17] examined reactions of Fe^+, Co^+, and Ni^+ with several alkyl halides. They postulated oxidative addition of the metal ion to the alkyl halide bond and were able to place limits on several M^+–R and M^+–X bond energies including $D°(Co^+–CH_3)$ and $D°(Co^+–I)$ which were $56.0 < D°(Co^+–CH_3) < 69.0$ kcal/mol and $D°(Co^+–I) > 56$ kcal/mol. In these studies, Fe^+, Co^+, and Ni^+ were formed by electron impact on $Fe(CO)_5$, $Co(CO)_3NO$, and $Ni(CO)_4$, respectively. Atomic transition metal ions formed by electron impact are formed in a mixture of ground and excited states, and the excited state population is a strong function of the electron energy, increasing rapidly with increasing electron energy up to 40–50 eV.[18] Aware of possible effects of excited state metal ions on these reactions, Fisher et al.[19] measured the absolute cross sections as a function of translational energy for Fe^+, Co^+, and Ni^+ reacting with CH_3X (X = Cl, Br, I) using surface ionization to produce the metal ions. With surface ionization (SI) a Boltzmann distribution of ground and excited states is produced. With a filament temperature of 2250 K, SI of $CoCl_2$ produces 85% a^3F ground state Co^+ and 15% a^5F excited state Co^+. Even though the effect of the 15% excited state Co^+ on the $Co^+ + CH_3I$ reaction cross section was not clearly delineated, previous studies[20] indicated that the $CoCH_3^+ + I$ channel was in fact endothermic on the ground state surface and on this basis a 298 K bond energy for Co^+–CH_3 was determined to be 51.2 $\pm$ 1.5 kcal/mol.[21] The CoI^+ channel was assumed to be exothermic on the ground state surface and therefore its bond energy was not derived. Two reaction mechanisms were proposed for the formation of CoI^+. At low energy, oxidative addition of Co^+ to the methyl iodide bond produces an inserted I–Co^+–CH_3 intermediate which subsequently dissociates to form either $CoCH_3^+$ or CoI^+. At high energy a direct mechanism producing only CoI^+ was proposed.

At this point several questions need to be addressed. What is the effect of the 15% excited state Co^+ on the $Co^+ + CH_3I$ cross

(1) For a recent review, see: Eller, K.; Schwarz, H. *Chem. Rev.* **1991**, *91*, 1121 and references therein.
(2) *Gas Phase Inorganic Chemistry*; Russel, D. H., Ed.; Plenum Press: New York, 1989.
(3) *Bonding Energetics in Organometallic Compounds*; Mark, T. J., Ed.; ACS Symp. Ser. 428; American Chemical Society: Washington, DC, 1990.
(4) van Koppen, P. A. M.; Kemper, P. R.; Bowers, M. T. *J. Am. Chem. Soc.* **1992**, *114*, 1083. van Koppen, P. A. M.; Kemper, P. R.; Bowers, M. T. *J. Am. Chem. Soc.* **1992**, *114*, 10941.
(5) Armentrout, P. B. *Science* **1991**, *251*, 175.
(6) Armentrout, P. B. *Annu. Rev. Phys. Chem.* **1990**, *41*, 313 and references therein.
(7) Hanton, S. D.; Noll, R. J.; Weisshaar, J. C. *J. Phys. Chem.* **1990**, *94*, 5655.
(8) Weisshaar, J. C. In *Advances in Chemical Physics*; Vol. 81, Ng, C., Ed.; Wiley-Interscience: New York, 1992; Vol. 81, and references therein.
(9) Armentrout, P. B. In *Gas Phase Inorganic Chemistry*; Russel, D. H., Ed.; Plenum Press: New York, 1989.
(10) Elkind, J. L.; Armentrout, P. B. *J. Phys. Chem.* **1986**, *90*, 5736.
(11) Elkind, J. L.; Armentrout, P. B. *J. Phys. Chem.* **1987**, *91*, 2037.
(12) (a) Sunderlin, L. S.; Aristov, N.; Armentrout, P. B. *J. Am. Chem. Soc.* **1987**, *109*, 78. (b) Aristov, N.; Armentrout, P. B. *J. Am. Chem. Soc.* **1986**, *108*, 1806.
(13) Sanders, L.; Hanton, S.; Weisshaar, J. C. *J. Phys. Chem.* **1987**, *91*, 5145.
(14) Sanders, L.; Hanton, S. D.; Weisshaar, J. C. *J. Chem. Phys.* **1990**, *92*, 3498.
(15) Freas, R. B.; Ridge, D. P. *J. Am. Chem. Soc.* **1980**, *102*, 7129. Reents, W. D., Jr.; Strobel, F.; Freas, R. B., III; Ridge, D. P. *J. Phys. Chem.* **1985**, *89*, 5666.
(16) Halle, L. F.; Armentrout, P. B.; Beauchamp, J. L. *J. Am. Chem. Soc.* **1981**, *103*, 962.
(17) Allison, J.; Ridge, D. P. *J. Am. Chem. Soc.* **1979**, *101*, 4998.
(18) (a) Kemper, P. R.; Bowers, M. T. *J. Phys. Chem.* **1991**, *95*, 5134. (b) Kemper, P. R.; Bowers, M. T. *J. Am. Chem. Soc.* **1990**, *112*, 3231.
(19) Fisher, E. R.; Sunderlin, L. S.; Armentrout, P. B. *J. Phys. Chem.* **1989**, *93*, 7375. Fisher, E. R.; Schultz, R. H.; Armentrout, P. B. *J. Phys. Chem.* **1989**, *93*, 7382.
(20) Georgiadis, R.; Fisher, E. R.; Armentrout, P. B. *J. Am. Chem. Soc.* **1989**, *111*, 4251.
(21) Only the $Co^+ + CH_3I$ and $Co^+ + CH_3Br$ data are used in referencing the bond energy determined by Fisher et al. because the other systems involved a significant kinetic shift in the threshold. Specifically, $D°(Co^+–CH_3)$ measured for Co^+ reacting with ethane, propane, isobutane, and neopentane decreased as the reactant neutral size increased (49.1, 46.9, 38, and 39 kcal/mol, respectively).[20] The larger the neutral, the greater the kinetic shift. Hence, these numbers should not be included in reporting the Co^+–CH_3 bond energy.

0002-7863/93/1515-5616$04.00/0

section data? Is the $CoCH_3^+$ channel in fact endothermic and the CoI^+ channel exothermic on the ground state surface? Is the bond energy derived for Co^+–CH_3 correct and what is the Co^+–I bond energy? Finally, does the mechanism involve a direct reaction at high energy and complex formation at low energy for the CoI^+ channel? Does only complex formation occur in the $CoCH_3^+$ channel?

These questions are addressed here by directly studying the interaction of the a^3F, a^5F, and b^3F states of Co^+ with CH_3I. The elimination and adduct formation reaction rate constants (and their temperature dependencies) are measured for both the ground and excited states of Co^+. By modeling the reaction efficiencies for the elimination channels on the ground state surface with statistical phase space theory,[22,23] the Co^+–CH_3 and Co^+–I bond energies are determined.

Experiment and Theory

Details of the instrument used in these experiments have been described[24] and are only briefly outlined here. The instrument couples a reverse-geometry mass spectrometer operating at 5 kV to a high-pressure, temperature-variable drift cell that operates at thermal energies. The first-stage mass spectrometer is a home-built instrument with the same dimensions and ion optics as a V.G. Instruments ZAB-2F. Co^+ ions are formed by electron impact on $Co(CO)_3NO$ and $CoCp(CO)_2$ or by surface ionization of $CoCl_2$ using a V.G. Instruments electron impact ionization source which was modified to do surface ionization. Upon exiting the source, the ions are accelerated to 5 kV and mass selected using the double focusing reverse geometry mass spectrometer. The ions are then decelerated to 2–3 eV kinetic energy and are focused and injected into the high-pressure drift cell containing 1.75 Torr of helium buffer gas. The ions are quickly thermalized by collisions with He and drift through the reaction cell at constant velocity due to the presence of a uniform drift field. The ions react with a trace ($\sim 2 \times 10^{-5}$ Torr) of CH_3I present in the He, exit the cell, and are quadrupole mass analyzed and detected. Reaction times typically range from 200 to 600 μs corresponding to drift fields of $E/N \leq 3.5 \times 10^{-17}$ V·cm^2. These fields do not perturb the ion translational temperature more than a few degrees.[24] However, we can increase the field to translationally excite the ions. The effect of the ion drift velocity on the temperature of the ions can be represented by a change in an "effective temperature",[25-27] T_{eff}, as indicated in eq 1, where

$$T_{eff} = T + \frac{M_r}{3k} v_d^2 \left[\frac{M_i + M_b}{M_i + M_r}\right] \quad (1)$$

T is the thermodynamic temperature, M_b is the mass of the buffer gas, v_d is the ion drift velocity, M_r is the mass of the reactant, M_i is the mass of the ion, and k is Boltzmann's constant. By increasing the drift field in our experiment, effective temperatures of 300–650 K could be used.

The electronic state populations are largely obtained from the ion arrival time distribution (ATD). The ATD for Co^+ is measured by pulsing the mass selected ion beam into the drift cell (pulse width $\sim$1–3 μs). The pulse simultaneously triggers a time-to-pulse-height converter ramp. Ions that exit the cell are collected as a function of time, giving the arrival time distribution. Ions that have different mobilities have different drift times through the cell and appear as different peaks in the ATD. With Co^+ the ground $3d^8$ configuration and the excited $4s3d^7$ configuration are well-separated in the ATD. This allows a direct determination of the $3d^8$ ground and $4s3d^7$ excited electronic state population. No excited state deactivation was observed. There are two excited states with $4s3d^7$ configurations present in Co^+ formed by electron impact, and additional information from the reaction was required to determine the state populations. This point is discussed below.

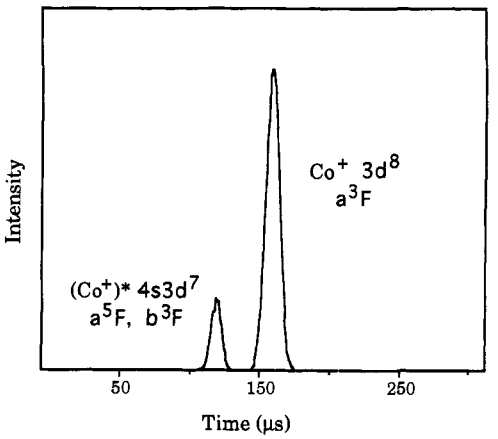

Figure 1. Co^+ arrival time distribution (ATD) [300 K, 50 eV electron energy, Co^+ from $CoCp(CO)_2$]. The absence of Co^+ arrival times intermediate between those of the excited state and ground state indicates deactivation does not occur from the excited state to the ground state. The integrated peak areas equal the populations of the electronic state configurations.

The state specific rate constants are determined by studying the reaction as a function of the state populations. The kinetics, which are solved in Section II, indicate that under the low conversion conditions of our experiment the fractional decrease $[Co^+]/[Co^+]_0$ is a simple exponential decay. The electronic state populations are altered by changing both the electron energy and the precursor used, ranging from 36 to 97% ground state Co^+. With the electronic state population determined, the $[Co^+]/[Co^+]_0$ ratio is measured as a function of time to obtain the total rate constant, k_{tot}. We measure k_{tot} as a function of percent ground state Co^+ and extrapolate to 100% ground state and 100% excited state Co^+ to determine the relative rates of reaction. Product distributions are measured as a function of percent ground state Co^+ to obtain individual rate constants.

The accuracy of the absolute total rate coefficient measurements is estimated to be within ±30%.[24] The relative rate coefficient measurements, however, are much more accurate (±10%).

Additional information regarding individual electronic state reactivities is obtained from product ion ATDs. In these experiments Co^+ is pulsed into the cell, but a particular product ion is collected instead of the bare metal ion. These product ATDs have separate components corresponding to the reaction of the $3d^8$ or $4s3d^7$ configurations to form the particular product. This method provides a separate, semiquantitative determination of the relative efficiencies with which the Co^+ states react to form the product ion. The use of this technique is discussed below.

The experimental reaction efficiencies for the elimination channels were modeled using statistical phase space theory. The parameters are well-defined for these reactions with frequencies and geometries obtained from ab initio calculations by Bauschlicher.[28] The only unknown parameters are the heats of formation of the $CoCH_3^+$ and CoI^+ product ions. By modeling the experimental reaction efficiencies, the overall heats of reaction and the Co^+–CH_3 and Co^+–I bond energies are determined. Details of the calculations and the parameters used are summarized in the Appendix.

Results

I. Arrival Time Distributions. (a) Electronic State Populations. A typical ATD for Co^+ is shown in Figure 1. Two peaks are observed corresponding to ground ($3d^8$) and excited ($4s3d^7$) electronic state configurations. The excited state Co^+ contains a 4s electron which is larger and more repulsive than the ground state which contains only 3d electrons.[18] The reduced attraction to He gives the excited state Co^+ a greater mobility than the ground state, causing the excited state to appear earlier in the

(22) (a) Pechukas, P.; Light, J. C.; Rankin, C. *J. Chem. Phys.* **1966**, *44*, 794. (b) Nikitin, E. *Theor. Exp. Chem. (Engl. Transl.)* **1965**, *1*, 285.
(23) (a) Chesnavich, W. J.; Bowers, M. T. *J. Am. Chem. Soc.* **1976**, *98*, 8301. (b) Chesnavich, W. J.; Bowers, M. T. *J. Chem. Phys.* **1978**, *68*, 901. (c) Chesnavich, W. J.; Bowers, M. T. *Prog. React. Kinet.* **1982**, *11*, 137.
(24) Kemper, P. R.; Bowers, M. T. *J. Am. Soc. Mass Spectrom.* **1990**, *1*, 197.
(25) (a) Ellis, H. W.; et al. Transport Properties of Gaseous Ions Over a Wide Range. In *At. Nucl. Data Tables* **1976**, *17*, 177; **1978**, *22*, 179; **1984**, *31*, 113. (b) Lindinger, W.; Albritton, D. C. *J. Chem. Phys.* **1975**, *62*, 3517.
(26) McFarland, M.; Albritton, D. C.; Fehsenfeld, F. C.; Ferguson, E. E.; Schmeltekopf, A. L. *J. Chem. Phys.* **1976**, *59*, 6610.
(27) McDaniel, E. W.; Mason, E. A. *The Mobility and Diffusion of Ions in Gases*; Wiley: New York, 1973.
(28) Bauschlicher, C. W., Jr., private communication.
(29) The time used in the analysis corresponds to ground-state Co^+. The extrapolated rate constant for excited-state Co^+ (0% ground state in Figure 4) is corrected for the shorter reaction time for excited-state Co^+. These corrected values are listed in Table I.

ATD than the ground state. The two peaks are baseline resolved. The absence of Co^+ ions with arrival times intermediate between those of the excited and ground state indicates deactivation does not occur from the excited state to the ground state while the ion traverses the reaction cell. Since deactivation does not occur, the integrated ATD peak areas equal the populations of the electronic configurations.

The peak corresponding to the $3d^8$ electronic configuration has been shown to contain only the ground state.[4] The excited state however has been shown to be a composite of the a^5F and b^3F states, both of which have a $4s3d^7$ electronic configuration.[4] To obtain information regarding the individual reactivity of the a^5F state with methyl iodide, Co^+ was formed by surface ionization of $CoCl_2$. Unlike electron impact, surface ionization of $CoCl_2$ on a resistively heated rhenium ribbon at approximately 2250 ± 100 K does not have enough energy to form measurable amounts of the b^3F second excited state. The electronic state population obtained by integrating the ATD peak areas is 15 ± 1% a^5F first excited state and 85 ± 1% a^3F ground state, in agreement with the calculated Boltzmann distribution at this temperature. The a^5F state formed by surface ionization was found to react with methyl iodide at a rate very similar to that of the combined b^3F and a^5F states formed by electron impact (the product ATDs were very similar for Co^+ formed by electron impact and surface ionization—see the following section). Consequently, the presence of any a^5F Co^+ in the electron impact experiments will have a negligible effect on our reported $Co^+(b^3F) + CH_3I$ rate constants, although the reported fraction of b^3F will be in error.

(b) Product Ion Peak Shapes. The product ATD for $CoCH_3^+$ is shown in Figure 2a. The observed peak is broad and consists of two components. The onset of these components correlates exactly to the ATDs of ground state Co^+ and excited state $(Co^+)^*$ as indicated by the dashed arrows (see Figure 2b). We interpret this result as follows. The arrival time for a particular $CoCH_3^+$ product ion is a function of the position at which it was formed in the cell. If Co^+ reacts with CH_3I at the end of the cell, the arrival time of the product $CoCH_3^+$ will correspond to the arrival time of Co^+. The longest $CoCH_3^+$ arrival times correspond to the formation of $CoCH_3^+$ at the entrance of the cell ($CoCH_3^+$ is larger and drifts more slowly through the helium in the cell than Co^+). The longest arrival time for the $CoCH_3^+$ product is the same for the excited state $(Co^+)^*$ as it is for ground state Co^+ in their reaction with CH_3I since the decrease in mobility due to the CH_3 ligand is much greater than the difference in mobility due to the different electronic state configurations. Hence the excited state $(Co^+)^*$ contribution to the $CoCH_3^+$ ATD goes all the way across the distribution as shown by the shaded area in Figure 2b.[4] Ions which react at intermediate positions in the cell have intermediate arrival times giving rise to the broad flat-topped peak we observe.

The observed shapes of the product ATDs are complicated by the presence of excited and ground state Co^+. However, the ATDs for both the ground and excited state reactions to form the $CoCH_3^+$ can be calculated from known transport properties and are expected to be broad and to decrease in intensity at long times. On the basis of this, as well as experimentally observed peak shapes where a single state dominates the reaction, we approximate the peak shape indicated by the shaded area for excited state $(Co^+)^*$ reacting to form the $CoCH_3^+$ product ion (denoted as $(Co^+)^*CH_3$ in Figure 2). Since the initial Co^+ beam consisted of 90% ground state Co^+ and 10% excited state $(Co^+)^*$, it appears from the relative areas in Figure 2a that ground state Co^+ forms the $CoCH_3^+$ product ion about as efficiently as the excited state does at 300 K.

The ATD for the CoI^+ channel is shown in Figure 3. Again there are two components in the ATD corresponding to the ground and excited states of Co^+ reacting with CH_3I to form the CoI^+. Unlike the $CoCH_3^+$ channel, the excited state is much more

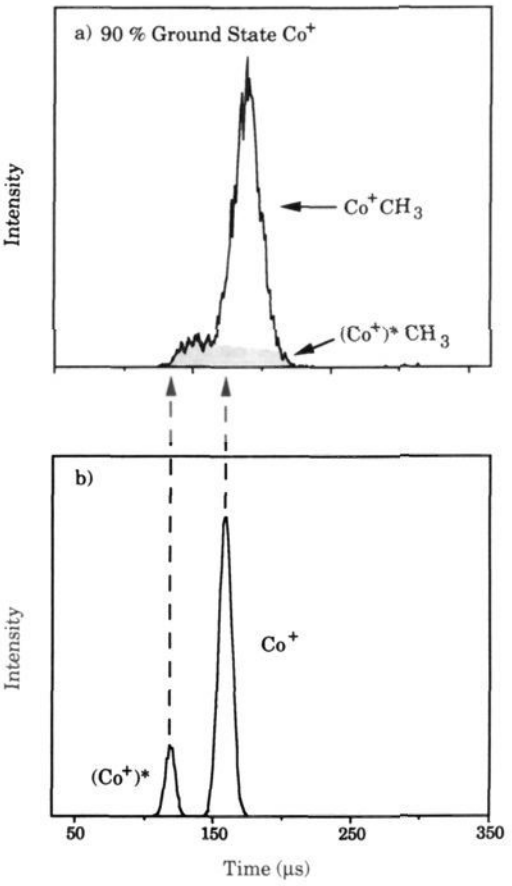

Figure 2. (a) Product ATD for $CoCH_3^+$ formed in the reaction of ground and excited states of Co^+ with CH_3I. The data shown are for a Co^+ ion beam containing 90% ground state Co^+ and 10% excited state $(Co^+)^*$. This beam is injected into the reaction cell where it reacts with CH_3I to form $CoCH_3^+$. The arrival time of the $CoCH_3^+$ product ion is a function of the position at which the reaction took place in the cell. The product ion peak shapes are discussed in the text, Section Ib. The contribution due to excited state reaction corresponds to the shaded area and is denoted as $(Co^+)^*CH_3$ (this notation does not imply excited state products are formed).

efficient in producing CoI^+ than the ground state over the temperature range measured from 300 to 650 K. In Figure 3a where the initial Co^+ beam consisted of 89% ground state and the effective temperature is 350 K, the ground state contribution to the CoI^+ ATD is less than 10% as indicated by the shaded area. As we increase the effective temperature from 350 to 650 K, the ground state contribution increases relative to the excited state contribution as indicated by the relative areas in Figure 3b. However, the excited state is still much more efficient than the ground state in producing CoI^+. These product ion ATDs suggest that CoI^+ product formation is more endothermic than $CoCH_3^+$ formation for ground state Co^+.

II. Kinetics and Reaction Rate Constants. The mechanism assumed for Co^+ reacting with CH_3I involves the formation of an internally excited $(CoCH_3I^+)^*$ complex which can be stabilized by collisions with helium, dissociate back to reactants, or eliminate I or CH_3.

Scheme I

$$Co^+ + CH_3I \underset{k_b}{\overset{k_f}{\rightleftharpoons}} (CoCH_3I^+)^* \xrightarrow{k_s(He)} CoCH_3I^+$$

$$(CoCH_3I^+)^* \xrightarrow{k'} CoCH_3^+ + I$$

$$(CoCH_3I^+)^* \xrightarrow{k'} CoI^+ + CH_3$$

For one electronic state of Co^+ the fractional decrease $[Co^+]/$

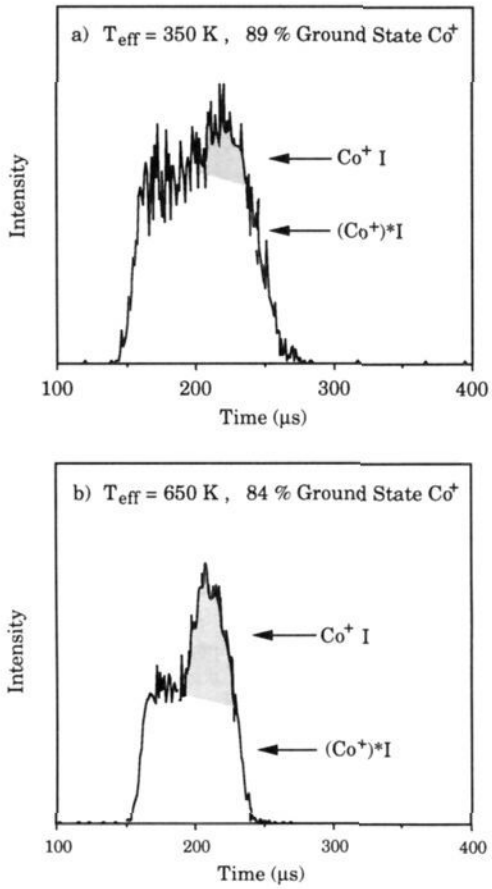

Figure 3. Product ATD for CoI^+ formed in the reaction of Co^+ with CH_3I at (a) 350 and (b) 650 K. For the Co^+ ion beam containing 89% ground state Co^+ and 11% excited state $(Co^+)^*$, the ground state contribution, indicated by the shaded area, is shown to increase with an increase in temperature. The relative areas for the ground and excited state contributions indicate the excited state is more efficient than the ground state in producing CoI^+.

$[Co^+]_0$ is a simple exponential decay as shown in eq (2). There

$$Co^+ \approx (Co^+)_0 e^{-k_{tot}t}, \quad k_{tot} = \frac{k_f k_s(He) + k' k_f}{k_b + k_s(He) + k'}(CH_3I) \qquad (2)$$

are, however, two electronic states of Co^+ with different reaction rates giving rise to the sum of two exponentials shown in eq 3.

$$Co^+ = f(Co^+)_0 e^{-k_{gs}t} + (1-f)(Co^+)_0 e^{-k_{ex}t} \qquad (3)$$

In this expression, Co^+ corresponds to the sum of ground and excited state Co^+, f is the fraction of ground state Co^+, and k_{gs} and k_{ex} are the ground and excited state rate constants, respectively. In the low conversion limit used in our experiments, the exponential decay of both ground and excited state Co^+ is well-described by linear functions (i.e. $e^{-kt} \cong 1 - kt$ for $kt \ll 1$). In this case, the sum of the two exponentials in eq 3 effectively reduces to the single exponential decay as given in eq 4. We

$$Co^+/(Co^+)_0 = e^{-k_{tot}t}, \quad k_{tot} = fk_{gs} + (1-f)k_{ex} \qquad (4)$$

obtain k_{tot} by plotting ln $[Co^+/(Co^+)_0]$ versus time. The total rate constant (k_{tot}), at 300 K and 1.75 Torr of He, for Co^+ reacting with CH_3I as a function of percent ground state Co^+ is shown in Figure 4. The experimental data points range from 39 to 97% ground state Co^+. A linear least-squares fit of the data points is used to determine the rates of reaction corresponding to 100% ground state and 100% excited state Co^+. The time used in the analysis corresponds to ground state Co^+. The extrapolated rate

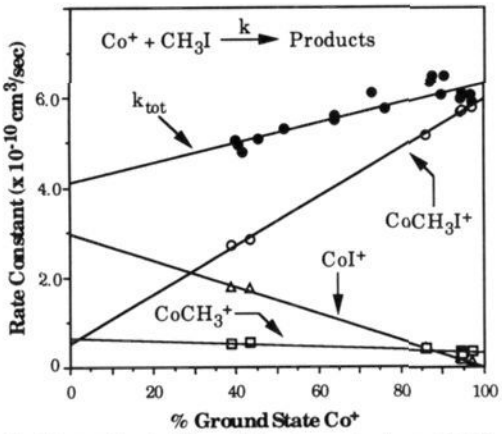

Figure 4. *The total and differential rate constants, at 300 K and 1.75* Torr of He, as a function of percent ground state Co^+. The linear least-squares fit of the experimental data points is used to extrapolate to rates of reaction corresponding to 100% ground state and 100% excited state Co^+.[29]

Table I. Effective $Co^+ + CH_3I$ Bimolecular Rate Constants at 300 K, 1.75 Torr of He[a]

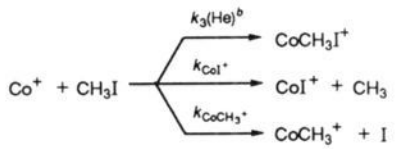

	$k_3(He)^c$	$k_{CoI^+}{}^c$	$k_{CoCH_3^+}{}^c$	$k_{tot}/k_{ADO}{}^d$	$k_{CoI^+}/k_{CoCH_3^+}$
Co^+ (a^3F, $3d^8$)	6.0	<0.05	0.34	0.48	<0.15
$(Co^+)^*$ (a^5F, b^3F, $4s3d^7$)	0.75[e]	4.4[e]	0.97[e]	0.46	4.5

[a] The accuracy of the absolute rate coefficient measurements is estimated to be within 30%.[24] The relative rate coefficient measurements, however, are much more accurate (±10%). [b] Only He stabilization is important due to the low CH_3I pressure. [c] Rate constants in units of 10^{-10} cm^3/s. [d] The average dipole orientation rate constant, $k_{ADO} = 1.33 \times 10^{-9}$ cm^3/s. [e] See ref 29.

constant for excited state Co^+ (0% ground state in Figure 4) is corrected for the shorter reaction time for excited state Co^+. These corrected values are listed in Table I.

Rate constants for adduct formation as well as CH_3 and I elimination are also shown in Figure 4 and are summarized in Table I. For the Co^+ a^3F $3d^8$ ground state reacting with CH_3I, adduct formation is the most abundant channel with a rate constant of 6.0×10^{-10} cm^3/s. The rate constants for the $CoI^+ + CH_3$ and $CoCH_3^+ + I$ channels are an order of magnitude lower with rate constants of $<0.5 \times 10^{-11}$ and 3.4×10^{-11} cm^3/s, respectively. For the Co^+ a^5F and b^3F excited states ($4s3d^7$ configuration) the elimination channels are enhanced. CoI^+ is the most abundant channel with a rate constant of 4.4×10^{-10} cm^3/s. This is a factor of 4.5 larger than the observed rate constant for $CoCH_3^+$ production (9.7×10^{-11} cm^3/s). The rate of adduct formation for the combined a^5F, b^3F $4s3d^7$ excited states of Co^+ is 7.5×10^{-11} cm^3/s, a factor of 8 less efficient than that for the a^3F $3d^8$ ground state Co^+. The factor of 8 difference in the adduct formation rate constants will change with the pressure of helium since the He pressure dependence of the apparent second-order rate constant differs for the different states. In the high-pressure (saturated) limit both ground and excited states will react to form the adduct at the collision rate. However, at 1.75 Torr of helium, the rate constant for adduct formation for the ground state is 45% of the collision limit, whereas the excited state forms the adduct at only 6% of the collision limit.

III. Co^+–I and Co^+–CH_3 Bond Energies. By modeling the experimental reaction efficiencies for the elimination channels on the ground state surface using statistical phase space theory, the overall heats of reaction and the bond energies for Co^+–CH_3

Table II. Reaction Thermochemistry by Theoretically Modeling the Experimental Reaction Efficiencies

$$Co^+ + CH_3I \rightarrow CoCH_3^+ + I$$
$$Co^+ + CH_3I \rightarrow CoI^+ + CH_3$$

	ground state Co^+ reaction efficiency, k/k_{ADO}		$D°_0$	ΔH_{rxn}
	experiment	theory	(kcal/mol)	(kcal/mol)
Co^+–CH_3	0.026	0.026	53.3 ± 2[a]	+1.9
Co^+–I	<0.001	0.00014	50.6 ± 2[a]	+4.6

[a] The uncertainty indicated corresponds to a factor of 10 increase or decrease in the theoretical reaction efficiency which is much larger than the uncertainty in the experimental reaction efficiency.

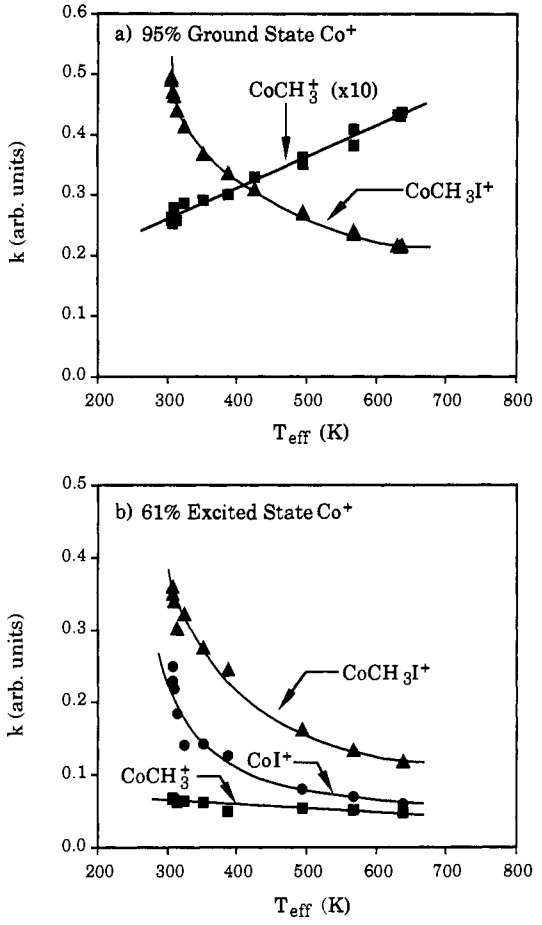

Figure 5. $CoCH_3I^+$, $CoCH_3^+$, and CoI^+ rate constants as a function of temperature for the Co^+ ion beam containing (a) 95% ground state Co^+ and (b) 61% excited state $(Co^+)^*$. The CoI^+ channel is not shown for 95% ground state Co^+ since the 5% excited state $(Co^+)^*$ dominates the reaction and a net negative temperature dependence is observed. The positive temperature for CoI^+ formation on the ground state surface is clearly seen in the product arrival time distributions shown in Figure 3.

and Co^+–I can be determined. Both channels were found to be endothermic, +1.9 and +4.6 kcal/mol for the $CoCH_3^+$ + I and CoI^+ + CH_3 channels, respectively. The Co^+–CH_3 and Co^+–I bond energies were determined to be $D°_0$ = 53.3 ± 2 and 50.6 ± 2 kcal/mol, respectively. Details of the calculations and the parameters which were used are outlined in the Appendix.

IV. Temperature Dependence of the Rate Constants. The rate constants for adduct formation as well as the elimination channels were measured as a function of effective temperature ranging from 300 to 650 K. A negative temperature dependence was observed for adduct formation for ground state Co^+ as shown in Figure 5a. This is not surprising since the probability for dissociation back to reactants increases with increasing temperature. A positive temperature dependence of the rate constants was observed for both $CoCH_3^+$ + I and CoI^+ + CH_3 channels on the ground state surface as shown in Figure 5a for the $CoCH_3^+$ channel and in Figure 3 for the CoI^+ channel. A positive temperature dependence is consistent with the fact that these reactions were found to be slightly endothermic. For excited state Co^+ a negative temperature dependence was observed for all three channels as shown in Figure 5b. The temperature dependence shown is for 61% excited state $(Co^+)^*$ and 39% ground state Co^+. This is the highest percentage of excited state we can produce experimentally. For 100% excited state $(Co^+)^*$, the temperature dependence of the rate constants would be even more negative for the elimination channels, particularly for the $CoCH_3^+$ channel. In this case the ground state reacts about as efficiently as the excited state but exhibits a positive temperature dependence. The true magnitude of the negative temperature dependence of the Co^+ excited state is hidden in the data with the ground/excited state mixture shown in Figure 5b.

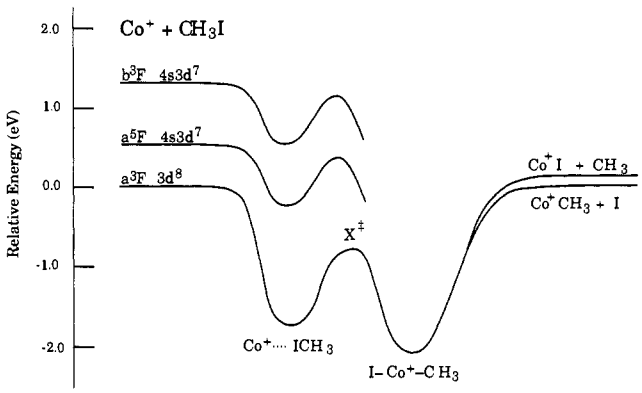

Figure 6. Schematic reaction coordinate diagram for the a^3F, a^5F, and b^3F states of Co^+ reacting with CH_3I.

Discussion

I. Reaction Mechanism and Energetics. A simplified schematic reaction coordinate diagram, consistent with all the data, is shown in Figure 6. Reactions of the a^3F $3d^8$ ground state Co^+ as well as the a^5F and b^3F $4s3d^7$ excited states of Co^+ with CH_3I are shown.

On the ground state surface, Co^+ and CH_3I react to form the Co^+···ICH_3 electrostatic complex. Oxidative addition of the cobalt ion to the methyl iodide bond yields the I–Co^+–CH_3 inserted intermediate[30] which dissociates to form the CoI^+ + CH_3 or $CoCH_3^+$ + I products. The transition state for I–C bond activation, denoted as $X^‡$ in Figure 6, must be located well below the reactant and product energies for the following reasons. The transition state for C–H bond activation for Co^+ reacting with propane was determined to be located 0.11 eV below the asymptotic energy of the reactants.[31] Since methyl iodide has a permanent dipole moment, it is more attractive to Co^+ than propane which does not have a permanent dipole moment. In addition, the I–C bond strength is less than the C–H bond strength. Hence, with a deeper electrostatic well and a lower bond activation energy, the oxidative addition transition state, $X^‡$, for the Co^+ + CH_3I system must be well below that for the Co^+ + C_3H_8 system and therefore well below the reactant and product energies

(30) Allison and Ridge[17] obtained strong evidence for oxidative addition to the methyl iodide bond for Fe^+ reacting with CH_3I. They found that $FeCH_3I^+$ reacts with CD_3I to form $FeICD_3I^+$ + CH_3 exclusively; no $FeICH_3I^+$ + CD_3 was observed. Exclusive CH_3 elimination indicates a symmetric $Fe(CH_3I)(CD_3I)^+$ complex is not formed and the Fe^+ ion must insert into the I–C bond to form the I–Fe^+–CH_3 intermediate which reacts with CD_3I eliminating CH_3. Other first-row transition-metal ions, including Co^+, are expected to activate methyl iodide in a similar fashion.

(31) van Koppen, P. A. M.; Brodbelt-Lustig, J.; Bowers, M. T.; Dearden, D. V.; Beauchamp, J. L.; Fisher, E. R.; Armentrout, P. B. *J. Am. Chem. Soc.* **1991**, *113*, 2359; **1990**, *112*, 5663.

as shown in Figure 6. The rate-limiting transition state for both elimination channels is thus the orbiting transition state in the exit channel. This is consistent with the positive temperature dependence observed for these reactions.

In contrast to the ground state, a negative temperature dependence is observed for the a^5F and b^3F excited states of Co^+ for both adduct formation and elimination channels. Oxidative addition of the $4s3d^7$ excited states of $(Co^+)^*$ to the C–I bond correlates to an antibonding orbital of the complex formed if the reaction remains on the excited state surface.[12,32] Formation of the inserted I–Co^+–CH_3 intermediate must therefore correlate to the ground state surface. As a consequence, the overall reaction for excited state $(Co^+)^*$ reacting with CH_3I becomes exothermic for both $CoI^+ + CH_3$ and $CoCH_3^+ + I$ product channels and the C–I bond activation transition state must be the rate-limiting transition state for these channels. An increase in temperature would then favor dissociation back to reactants (through the orbiting transition state) over C–I bond activation (through a tight transition state). This occurs because the density of states increases more quickly with temperature for an orbiting than for a tight transition state.

The $CoI^+ + CH_3$ channel is observed to be favored over the $CoCH_3^+ + I$ channel for excited state $(Co^+)^*$ reacting with CH_3I. There are two possible mechanisms that can explain this effect. First, insertion of $(Co^+)^*$ into the C–I bond could occur as it does in the ground state via transition state I. The insertion transition

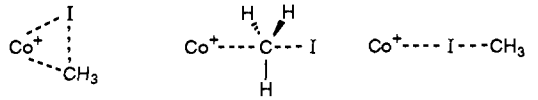

I II III

state I would be strongly mixed with the ground state, resulting in ground state $ICoCH_3^+$ which subsequently dissociates to form $CoI^+ + CH_3$ and $CoCH_3^+ + I$ products. In this mechanism the insertion transition state is overall rate determining but the branching ratio is determined by competition between the two orbiting transition states in the exit channel. In this case the $CoI^+ + CH_3$ channel will be favored over the $CoCH_3^+ + I$ channel due to its greater rotational density of states, a result in agreement with experiment and consistent with statistical phase space calculations (details given in the next section). Further, strong mixing of the ground state with the excited state in the insertion transition state greatly lowers the transition state energy, offsetting the fact that the $(Co^+)^*CH_3I$ electrostatic complex is much less strongly bound than the ground state complex (due to the repulsive 4s electron in the excited state $(Co^+)^*$) and the fact that the occupied 4s orbital of $(Co^+)^*$ impedes insertion from occurring. Finally, since a common tight transition state is rate limiting in this model, both channels should exhibit a negative temperature dependence, as observed.

The second mechanism was suggested by a reviewer. In this mechanism the branching ratio is determined by competition between the two "abstraction" transition states II and III. In both cases the C–I bond is "broken" in the transition state, but presumably transition state III is lower in energy than II due to the fact that the iodine atom is the negative end of the dipole in CH_3I and because the CH_3 group must invert when transition state II is involved. Exothermic abstraction predicts a negative temperature dependence for both channels since both go through a tight transition state whose energy is presumably lower than the $(Co^+)^* + CH_3I$ asymptotic energy. The $CoI^+ + CH_3$ products would be favored over $CoCH_3^+ + I$ since transition state III is expected to be lower in energy than transition state II.

There are, however, some serious problems with this "abstraction" mechanism. First, the excited electronic configuration of $(Co^+)^*$ is $4s3d^7$, and it is the 4s orbital that binds to the methyl or iodine in transition states II and III. As a consequence, the reaction retains excited state character in both the transition states and the products. Thus, it is not obvious that the reactions are exothermic in this mechanism since the ground state reactions of $Co^+ + CH_3I$ to form $CoCH_3^+ + I$ and $CoI^+ + CH_3$ are endothermic. Reactions occurring on the excited state surface may be even more endothermic because the occupied 4s orbital is expected to reduce the binding energy. Endothermic abstraction would exhibit a positive temperature dependence, and the reactions would be relatively inefficient (as observed for ground state Co^+ where $CoCH_3^+ + I$ and $CoI^+ + CH_3$ are formed at only 6% of the collision rate). This model is thus not consistent with experiment since a negative temperature dependence is observed and, for excited state $(Co^+)^*$, the $CoCH_3^+ + I$ and $CoI^+ + CH_3$ products are formed at 40% of the collision limit. Consequently, it is unlikely transition states II and III are involved in any significant way with the chemistry reported in this paper. Rather, we feel it is the strong mixing of the excited and ground state surfaces in transition state I which enhances the $CoCH_3^+ + I$ and $CoI^+ + CH_3$ channels for excited state $(Co^+)^*$ relative to the ground state Co^+ reactions.

The Co^+–CH_3 and Co^+–I bond energies, determined by modeling the reaction efficiencies for the elimination channels on the ground state surface, are $D°_0 = 53.3 \pm 2$ and 50.6 ± 2 kcal/mol, respectively. The Co^+–CH_3 bond energy is in good agreement with literature values. Fisher et al.[19] determined $D°_{298}(Co^+–CH_3)$ to be 51.2 ± 1.5 kcal/mol (converting to 0 K this value decreases to $D°_0 = 50.1 \pm 1.5$ kcal/mol), and Bauschlicher[33] calculated a lower limit of 48.3 kcal/mol. Allison and Ridge[17] determined these bond energies to be much higher, $56.0 < D°(Co^+–CH_3) < 69.0$ kcal/mol and $D°(Co^+–I) > 56$ kcal/mol. However, since electron impact ionization was used in these experiments, the effect of excited state $(Co^+)^*$ will be significant, yielding incorrect bond energies.

II. Reaction Rate Constants. Under the relatively high pressure conditions of our experiment (1.75 Torr of He), adduct formation represents 94% of the total ground state products. The elimination channels are relatively inefficient. The CoI^+ channel is essentially nonexistent at 300 K. The inefficiencies of these channels are consistent with the fact that both channels were found to be slightly endothermic and therefore do not compete effectively with collisional stabilization of the vibrationally excited $(CoCH_3I^+)^*$ complex (see Scheme I).

The rate constant data indicate that adduct formation for the $a^3F\ 3d^8$ ground state of Co^+ is more efficient than for the a^5F and $b^3F\ 4s3d^7$ excited states of Co^+. The repulsive 4s electron in the $Co^+\ 4s3d^7$ excited states greatly reduces the $(Co^+)^*$–ICH_3 well depth and therefore reduces the clustering efficiency of $(Co^+)^*$ with CH_3I. In addition, since oxidative addition of the $4s3d^7$ excited states of Co^+ to the C–I bond correlates to the ground state, the elimination channels are exothermic and effectively compete with collisional stabilization of the excited $(Co^+)^*CH_3I$ adduct.

Since the CH_3 and I elimination channels are both exothermic for the excited states of Co^+, they are enhanced relative to those of ground state Co^+. For the excited states of Co^+, the $CoI^+ + CH_3$ channel is favored over the $CoCH_3^+ + I$ channel due to the greater rotational density of states for the $CoI^+ + CH_3$ products relative to the $CoCH_3^+ + I$ products. Statistical phase space calculations are consistent with these results. Even though applying statistical phase space theory to a system where two surfaces are involved is not always possible, in this case it is. In the reaction of excited state $(Co^+)^* + CH_3I$, the rate-limiting transition state, C–I bond activation, is the same for both the $CoI^+ + CH_3$ and $CoCH_3^+ + I$ channels. It is at this transition

(32) Tonkyn, R.; Ronan, M.; Weisshaar, J. C. *J. Phys. Chem.* **1988**, *92*, 92.

(33) Bauschlicher, C. W., Jr.; Langhoff, S. R. *Int. Rev. Phys. Chem.* **1990**, *9*, 149.

state that the excited and ground state surfaces mix and formation of the $I–Co^+–CH_3$ intermediate correlates to the ground state surface. Subsequent dissociation of this complex leads to the $CoCH_3^+ + I$ and $CoI^+ + CH_3$ products. Phase space theory was used to calculate the probability for dissociation through the $CoCH_3^+ + I$ and $CoI^+ + CH_3$ orbiting transition states as a function of the available energy. The calculations indicate that the greater the available energy the more the $CoI^+ + CH_3$ channel is favored over the $CoCH_3^+ + I$ channel (simply due to the greater rotational density of states associated with the $CoI^+ + CH_3$ channel). Since the b^3F state is higher in energy then the a^5F state of Co^+, the $CoI^+/CoCH_3^+$ branching ratio will increase as the population of the b^3F state increases. Modeling the experimental $CoI^+/CoCH_3^+$ branching ratio for 100% excited state Co^+ using phase space theory indicates that the excited state population is about 74% b^3F and 26% a^5F. This population may vary with electron energy, introducing some uncertainty in the excited state rate constants.

Absolute reaction cross sections for methyl and iodide elimination channels have been measured by Fisher et al.[19] under single-collision conditions. In these experiments, surface ionization of $CoCl_2$ produces 85% a^3F ground state Co^+ and 15% a^5F excited state $(Co^+)^*$. At low kinetic energy, they observe the reaction to be exothermic for both the $CoCH_3^+$ and CoI^+ channels. The cross section drops off with increasing energy until approximately 1.5 eV where both the $CoCH_3^+$ and CoI^+ cross sections increase. Since previous studies by Georgiadis et al.[20] indicate the $CoCH_3^+$ I channel to be endothermic on the ground state surface, the exothermic behavior in the cross-section data was attributed to the 15% excited state $(Co^+)^*$ reaction and the high energy feature was attributed to the ground state Co^+ reaction. The $CoI^+ + CH_3^+$ channel was assumed to be exothermic on the ground state surface, and a direct mechanism was proposed to be responsible for the high-energy feature in the cross-section data. Since our data show both the $CoI^+ + CH_3$ and $CoCH_3^+ + I$ channels to be endothermic on the ground state surface, we believe the exothermic component in the cross-section data for both the CoI^+ and $CoCH_3^+$ channels at low kinetic energy is due to the 15% excited state Co^+. With increasing collision energy, the cross sections for both CoI^+ and $CoCH_3^+$ increase on the ground state surface and appear as high-energy features in the cross-section data for both channels.[19] At high collision energies a direct mechanism to form the $CoI^+ + CH_3$ could occur, but such a mechanism is not necessary to explain the observed results.

The $CoI^+/CoCH_3^+$ product ratio we observe for ground state Co^+ is <0.15. For the a^5F, b^3F excited states of Co^+ this ratio increases dramatically to 4.5. Under surface ionization conditions, where 15% a^5F excited state and 85% a^3F ground state Co^+ are formed, we observe this ratio to be 1.3, which as expected is intermediate between the results of the ground and excited states. In the surface ionization experiments of Fisher et al.,[19] the $CoI^+/CoCH_3^+$ ratio was observed to be 0.77 at low kinetic energy. This is somewhat lower but consistent with our results considering the fact that we are working under high-pressure, multicollision conditions, which overemphasizes contribution of the excited state elimination reactions[34] relative to the low-pressure, single-collision experiment of Fisher et al. elimination reactions[34] relative to the low-pressure, single-collision experiment of Fisher et al.

Conclusion

By measuring the rate constants as a function of temperature for the a^3F, a^5F, and b^3F states of Co^+ reacting with CH_3I, detailed insight into the mechanism and energetics of these reactions has been obtained. Under the high-pressure conditions of our experiments (1.75 Torr of He), adduct formation is the dominant product for the a^3F $3d^8$ ground state of Co^+, with only small amounts of elimination products observed. The a^5F and b^3F $4s3d^7$ excited states of Co^+ react similar to each other and show greatly reduced clustering efficiency but enhanced elimination relative to the ground state.

The temperature dependence of the rate constants indicates that all reaction channels for both ground and excited state Co^+ reacting with CH_3I involve the formation of a complex as the initial step in the reaction. Elimination proceeds via oxidative addition of the cobalt ion to the methyl iodide to form the $I–Co^+–CH_3$ intermediate which subsequently dissociates to form either the $CoCH_3^+$ or CoI^+ product ions.

Both methyl and iodide elimination channels were determined to be endothermic on the ground state surface by modeling the efficiencies of these reactions using statistical phase space theory assuming the rate-limiting transition state is the orbiting transition state in the exit channel. This result is consistent with the strong positive temperature dependence observed experimentally for these reactions. The bond energies determined for $Co^+–CH_3$ and $Co^+–I$ were $D°_0 = 53.3 \pm 2$ and 50.6 ± 2 kcal/mol, respectively, in good agreement with literature values for the $Co^+–CH_3$ bond energy. No literature values for the $Co^+–I$ bond energy are available.

For excited state $(Co^+)^*$ reacting with CH_3I, oxidative addition of the cobalt ion to the methyl iodide correlates to the ground state surface, resulting in the elimination channels becoming exothermic. The negative temperature dependence of the rate constant observed for both elimination channels for the excited state $(Co^+)^*$ reaction implies that in this case the C–I bond activation transition state is the rate-limiting transition state. The enhancement of the $CoI^+ + CH_3$ channel over the $CoCH_3^+ + I$ channel observed for both the a^5F and b^3F excited states of Co^+ was reproduced in the phase space calculations and is due to the greater rotational densities of states of the $CoI^+ + CH_3$ products.

Acknowledgment. The support of the National Science Foundation under Grant CHE91-19752 is greatfully acknowledged. We also thank Professors Peter Armentrout and Seung Koo Shin for several useful discussions and special thanks to Dr. Charles W. Bauschlicher, Jr., for calculating the geometries and frequencies summarized in Table III.

Appendix

The experimental reaction efficiencies for the $CoCH_3^+ + I$ and $CoI^+ + CH_3$ elimination channels were modeled using statistical phase space theory. In all instances the collision complex was formed through an orbiting transition state and dissociated to products via an orbiting transition state. The potential energy surface used in the calculations is shown in Figure 6. Competition occurs for the internally excited $(Co(CH_3I)^+)^*$ complex between stabilization by collisions with helium and dissociation back to reactants and to eliminating products via orbiting transition states.

The probability of a $Co(CH_3I)^+$ complex with energy E and angular momentum J forming products in channel i is given by expression A1, where $F^{orb}(E,J)$ is the microcanonical flux through

(34) Enhancement of the CoI^+ channel is expected under the multicollision conditions of our experiment. This is due to the fact that on the ground-state surface both methyl and iodide elimination channels are endothermic and collisional stabilization of the adduct is the dominant channel. That is, the elimination channels are very inefficient (<2% of the collision limit) and cannot compete effectively with adduct formation on the ground-state surface under multicollision conditions (adduct formation represents 94% of the total ground-state products whereas the elimination channels represent only 6%). On the excited-state surface, however, both elimination channels are exothermic and dominate over adduct formation (88% elimination versus 12% adduct formation) with the $CoI^+ + CH_3$ channel favored by a factor of 4.5 over the $CoCH_3^+ + I$ channel. Thus, under high-pressure conditions, with 15% excited-state $(Co^+)^*$, the $CoI^+/CoCH_3^+$ branching ratio (observed to be 1.3) tends to reflect that of the excited state (which is 4.5) rather than the ground state (<0.15) and is therefore somewhat larger than the branching ratio of 0.77 observed under single-collision conditions.

Table III. Input Parameters Used in Calculations

	Co^+	CH_3I	$CoCH_3^+$	CoI^+	CH_3	I
$\Delta H_f°_0$ [a]	282	6.0	264.3	257.0	35.6	25.6
B [b]		0.688	0.843	0.209	8.34	
σ [c]		3	3	1	6	
α [d]		6.3 (13.4)[e]			1.92	5.87
ν_i [f]		533	282	285	407	
		882 (2)	490		1389(2)	
		1252	532		2926	
		1432 (2)	1317		3085(2)	
		2933	1372			
		3060 (2)	1381			
			2891			
			3004			
			3032			

[a] Heat of formation at 0 K in kcal/mol. [b] Rotational constant in cm^{-1}. [c] Symmetry number. [d] Polarizability in $Å^3$. [e] The polarizability used in the calculations is the larger value in parentheses.[35] [f] Vibrational frequencies[27] in cm^{-1}.

$$P_i(E,J) = \frac{F_i^{\ddagger}(E,J)}{F^{orb}(E,J) + F_i^{\ddagger}(E,J) + F_j^{\ddagger}(E,J)} \quad \text{(A1)}$$

the orbiting transition state back to reactants and $F_i^{\ddagger}(E,J)$ and $F_j^{\ddagger}(E,J)$ are the fluxes through the orbiting transition states to go on to products in channels i and j, respectively. Averaging over the E,J distribution, the bimolecular rate constant for formation of product i, relative to the total collision rate constant, is given by expression A2. The reaction efficiencies calculated from eq A2 are used for comparison with the measured reaction efficiencies.

$$\frac{k_i}{k_{collision}} = \left[\int_0^{\infty} dE\, e^{-E/kT} \int_0^{J_{max}} dJ 2J\, F^{orb}(E,J) \times \frac{F_i^{\ddagger}(E,J)}{F^{orb}(E,J) + F_i^{\ddagger}(E,J) + F_j^{\ddagger}(E,J)} \right] / \left[\int_0^{\infty} dE\, e^{-E/kT} \int_0^{J_{max}} dJ 2J\, F^{orb}(E,J) \right] \quad \text{(A2)}$$

Stabilization of the $CoCH_3I^+$ complex by collisions with helium is not included in eq A2 because the effect on the overall reaction efficiencies for elimination channels was calculated to be negligible (a maximum of 0.7 kcal/mol increase in the bond energy was determined). This is not surprising considering the fact that the elimination reactions are slightly endothermic and only the $CoCH_3I^+$ collision complexes with relatively high internal energy will dissociate to form the $CoCH_3^+$ + I and CoI^+ + CH_3 elimination products and these high energy complexes are precisely the ones that have the least chance of collisional stabilization (short complex lifetime).

The parameters are well-defined for these reactions with frequencies and geometries obtained from ab initio calculations by Bauschlicher.[28] The only unknown parameters are the heats of formation of the $CoCH_3^+$ and CoI^+ product ions. By modeling the experimental reaction efficiencies, the overall heats of reaction and the Co^+–CH_3 and Co^+–I bond energies are determined. The parameters used in the calculations are summarized in Table III.

(35) The phase space calculations reported here employ the ion-induced dipole potential, $V(r) = -q^2\alpha/2r^4$. The potential is a good approximation for ion-molecule reactions where the neutral does not possess a permanent dipole moment. Since CH_3I does contain a permanent dipole moment, the Co^+/CH_3I long-range potential is more realistically represented by the ion-dipole potential, $V(r) = -q^2\alpha/2r^4 - (\mu_D q/r^2)\cos\theta$.[36,37] Even though this potential has yet to be included in the phase space calculations, increasing the polarizability of the neutral molecule has been shown[38] to approximate the increased ion-induced dipole attraction due to the presence of a permanent dipole moment in the neutral, giving good agreement between experiment and theory. The value of the polarizability used in the calculations was such that the calculated ion-induced dipole capture rate constant gives the same rate constant as that calculated from average dipole orientation (ADO) theory.[36,37]

(36) Su, T.; Bowers, M. T. *J. Chem. Phys.* **1973**, *58*, 3027.

(37) Su, T.; Bowers, M. T. In *Gas Phase Ion Chemistry*; Bowers, M. T., Ed.; Academic Press: New York, 1979; Vol. I.

(38) Illies, A. J.; Jarrold, M. F.; Bass, L. M.; Bowers, M. T. *J. Am. Chem. Soc.* **1983**, *105*, 5775.